

# Effect of Sintering Parameters on Physical Properties of SS 316L Alloy Compact

*Mohd Faizul Farhan Ahmad Hamidi*

*Institute of Postgraduate Studies, Universiti Malaysia Pahang,  
Lebuhraya Tun Razak, 26300 Gambang, Kuantan, Pahang, Malaysia*

*Wan Sharuzi Wan Harun*

*Saiful Anwar Che Ghani*

*Dayangku Noorfazidah Awang Shri*

*Human Engineering Group, Faculty of Mechanical Engineering,  
Universiti Malaysia Pahang, 26600 Pekan, Pahang, Malaysia*

*Toshiya Osada*

*Department of Mechanical Engineering, Kyushu University,  
Motooka 744, Nishi-ku, Fukuoka 819-0395, Japan*

## ABSTRACT

*Recently, metal injection moulding (MIM) has been identified as an economical fabrication technique for metal components. MIM, adapted from plastic injection moulding, has four major processing stages, which are: mixing of powder and binder system to produce feedstock, injection moulding, debinding and sintering. In this paper, the physical properties of SS 316L alloy sintered compact sintered at three different sintering parameters were discussed. Thermal properties of the feedstock were characterized by Thermogravimetric Analyzer (TGA) analysis. The debound compacts were sintered at 1100, 1200, and 1300 °C for 3 hours in the high pure argon atmosphere. The heating rate has been set at 10°C/min. The relative density, dimensional shrinkage and microstructure of the sintered compact were investigated. The relative density and dimensional shrinkage increased with the sintering parameters due to high densification of the sintered compact. Some pore sizes seemed to decrease with the increase in sintering temperature. Different sintering temperature shows a significant effect on the physical properties of the sintered compact.*

**Keywords:** *Metal Injection Moulding, Physical Properties, Microstructure*

## **Introduction**

Metal injection moulding (MIM) method is a relatively recent technology to create net shape parts in the powder metallurgy industry. There is nearly unlimited choice of material for this powder metallurgy technique and it integrates the design versatility of plastic injection moulding process [1, 2]. Furthermore, this processing method has received great attention in numerous applications such as biomedical, electrical tools and automotive industries [3]-[6]. Stainless steel 316L is the favourable material used in metal injection moulding process due to its good properties, either prepared in water or gas atomised. Its reputation stems from its abilities to sinter to high densities and achieve excellent corrosion resistance. This metal is also broadly used in MIM research field and industrial utilisations [7, 8].

In MIM technique, there are four consecutive steps which are mixing of binder and powder, injection moulding, extraction of binder, and sintering process that produce strong inter-particle bonds between powder particles [9, 10]. To achieve the quality for standard MIM parts, they should demonstrate excellent dimensional control and high density. Generally, the linear shrinkage of several MIM parts are varied between 10 to 20% [11]. In order to obtain the final parts with the requisite dimensional accuracy and physical properties, it is thus necessary to study the factors that affect the properties of the MIM parts. In all of the MIM processing stage, sintering is the most critical phase that influence the densification of the compact as well as physical and mechanical properties. Earlier research have found that the crucial parameters of the sintering process are heating rate, atmosphere, sintering temperature and soaking time. These parameters influence the microstructure, pore size and shape, and the densification of the sintered compact [12, 13].

The purpose of the present study is to investigate the effects of sintering parameters on the physical properties of MIM SS 316L alloy. The moulded test compacts are debound and sintered in a high pure argon atmosphere at three different sintering temperature. The sintered test compacts were characterised with regard to densification, dimensional shrinkage measurements, and microstructure. The compact that is sintered at higher sintering temperature is expected to give better densification, higher dimensional shrinkage and less number of porosity compared to others sintering temperature.

## **Experimental Set Up**

### **Material and Injection Moulding**

The 316L stainless steel alloy powder used in this work was supplied by Osprey Co, UK with the average size of 22  $\mu\text{m}$  were premixed in a 62/38 volume ratio which is based on a previous study. The chemical composition of

the powder is shown in Table 1. The binder system consists of 69% paraffin wax (PW), 20% polypropylene (PP), 10% carnauba wax (CW) and 1% stearic acid (SA) was used to prepare the feedstock. The twin blade type mixer was used to mixed the feedstock at a rotational speed of 70 rpm and mixing temperature of 150 °C for 90 min. A powder loading of 62 vol.% was used which is based on the optimum powder loading determined by a previous work. The thermal properties of the feedstock were analysed using thermogravimetric analysis.

Table 1: Chemical composition of SS 316L alloy powder

Element	Wt.%
Cr	16.7
Ni	10.3
Mo	2.2
Mn	0.99
Si	0.69
P	0.02
C	0.01
S	0.05

Injection moulding of the feedstock was carried out on a Nissei NS20-2A injection moulding machine to produce tensile shape compact with dimension as shown in Figure 1. The feedstock was injected at 150 °C under the pressure of 117 MPa and holding pressure of 58.5 MPa.

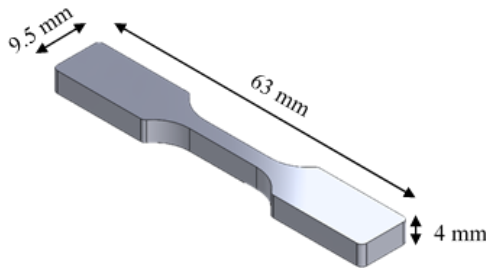


Figure 1: Dimension of tensile compact

### **Debinding and Sintering**

The green compact were then subjected to solvent debinding at 60 °C by keeping it in solvent bath of vaporised heptane for 2 h. For the thermal debinding stage, the debound compact was heated up to 500°C for 1 hour with heating rates of 5 °C/min in a high purity argon atmosphere. Moreover, the melt wicking debinding was applied by using fine Al<sub>2</sub>O<sub>3</sub> powders at this stage [14]. Next to the debinding stage, the sintering was performed at three different

temperatures from 1100 to 1300°C for 3 hours in a high purity argon atmosphere at a heating rate of 10 °C/min. The flow rate of argon was retained at 1.0 L/min.

### Characterisation of the Sintered Compacts

The sintered compacts were section into few pieces by using abrasive cutter blade. Water immersion technique was used to determine the relative density of each pieces of sintered compacts. The dimensional shrinkage was measured using Vernier calliper and the microstructure of the sintered compact was investigated using optical microscope (OM).

## Result and Discussion

### Thermal Curve for Feedstock

Thermal properties of the feedstock from the TGA test are shown in Figure 2. For this feedstock the remaining residue was 93.5 wt.%, which is equivalent to the remaining quantity of metal powder in the feedstock. The difference in the total decomposition of binder components from the calculated one is due to the few binder being left inside the mixer, which decreased its amount. During mixing and injection process, the temperature used should be lower than the decomposition temperature of the binder components to prevent binder loss. As seen in Figure 2, the decomposition temperature for the binder was started at 180°C and it can be concluded that the decomposition of binders has not occurred in the mixing and injection process as the temperature was set at 150°C for both processes. The three degradation slopes were observed at 180°C, 370 °C, and 430 °C which are related to all binder components in the feedstock. The first slope indicates the degradation process for paraffin wax and stearic acid, while the second and third slope indicates the degradation process for carnauba wax and polypropylene.

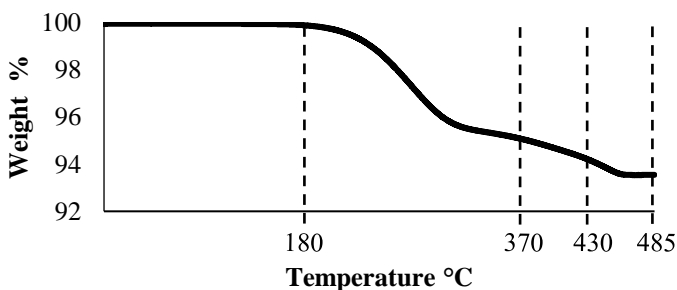


Figure 2: TGA curve of SS 316L alloy feedstock

### Effect of Sintering Parameter on Sintered Density

Figure 3 demonstrated the densification results of SS 316L alloy sintered compacts. The relative density varied between 85.5% and 88.2%. The relative density was increased by increasing the sintering temperature. From the result, 1100°C 3h recorded the lowest relative density compared to the relative density attained using others parameter. This was considered due to the presence of large number of pores observed clearly from the optical micrograph shown in Figure 6. Previous research has found that the sintered density for micro-powder SS 316L alloy compact increases rapidly in a temperature varied between 1100 to 1200 °C with an increase in density from 77 to 85% [8].

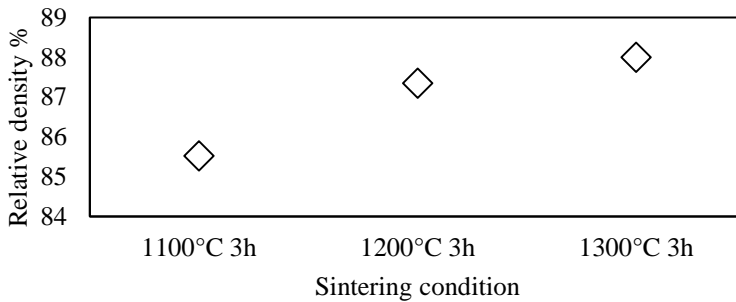


Figure 3: Relative density for SS 316L alloy sintered compact

### Effect of Sintering Parameter on Dimensional Shrinkage

The compacts experienced binder removal throughout thermal debinding and finally particle bonding in sintering, which affect the dimensional difference in the compact. Typically, the changes in dimension of a compact is known by the linear shrinkage ( $\Delta L/L_0$ ), where  $\Delta L$  is the dimensional change between the green compact and the sintered compact, and  $L_0$  is the dimension of the green compact. The dimensional shrinkage of the green and sintered compacts were measured from the changes in their dimensions as shown in Figure 4. The linear shrinkage of many MIM compacts are varied between 10 to 20 % [15]. However, the shrinkage recorded in this work are in the range of 8.0 to 9.9 %. A linear shrinkage of 10 to 20% can be achieved if the applied sintering temperature is more than 1300 °C. Previous work by [16] have found that the linear shrinkage of sintered compact will increase from 12 to 15% when the sintering temperature is increased from 1300 to 1360 °C. As seen in Figure 5, the shrinkage result rises with the increase in sintering temperature. During the sintering process, the particles start to diffuse and formed neck growth. As the sintering temperature increases, it develops the contact length among the particles through grain boundary diffusion, volume diffusion and plastic diffusion which also increase the linear shrinkage of the sintered compacts [7].



Figure 4: Compact dimensional difference between the green compact (below) and the sintered compact (upper)

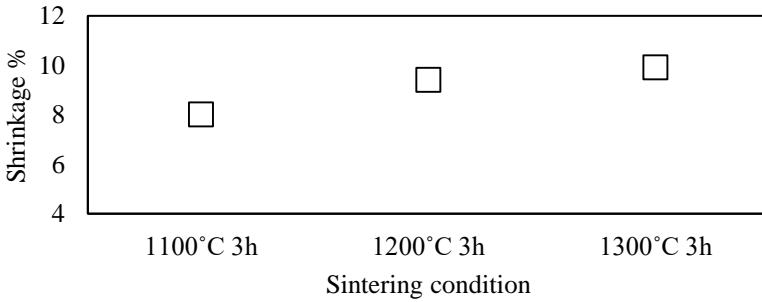


Figure 5: Shrinkage amount for sintered compact

### Effect of Sintering Parameter on Microstructure Observation

The microstructure of the compact sintered at different sintering temperature is further examined as in Figure 6. The microstructures represent an advancement from irregular to spherical pores followed by a tendency for pores to be segregated in their distribution by increasing the sintering temperature. It is obviously shown that the porosity decreases with increasing sintering temperature. A compact that was sintered at 1300 °C for 3 h demonstrates less pore size compared to other parameters. The presence of pores leads to the lowering of the compact's relative density which is due to low densification. This result can provide a strong evidence on why the relative density of compact sintered at 1300 °C for 3 h was greater than the other parameters.

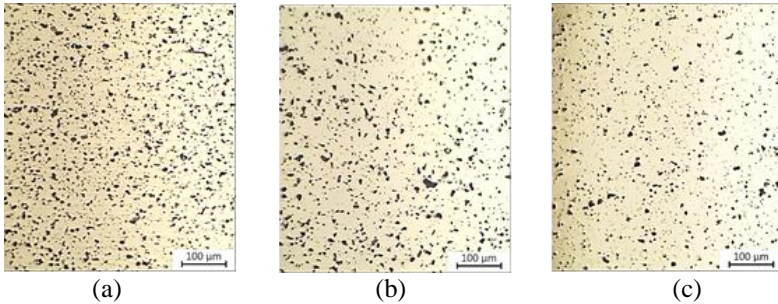


Figure 6: Optical micrograph of sintered compact at different conditions; (a) 1100°C 3h, (b) 1200°C 3h, (c) 1300°C 3h

## **Conclusion**

This work analysed the physical properties and microstructure properties of SS 316L alloy compact fabricated by metal injection moulding processes. The key findings include:

- (1) Based on TGA analysis, the degradation temperature of the binder started at 180°C and it can be concluded that the binders will not decompose during mixing and injection moulding process as the temperature for both process was set at 150 °C.
- (2) The relative density and dimensional shrinkage increased with an increase in the sintering temperature due to high densification of the sintered compact.
- (3) For microstructure observation, porosity decreases with increasing sintering temperature.

## **Acknowledgement**

The authors would like to express their appreciation to Universiti Malaysia Pahang through grant RDU151314 (Research Acculturation Collaborative Effort) and RDU150337 (UMP grant)

## **References**

- [1] H. Ö. Gülsoy, Ö. Özgün, and S. Bilketay, "Powder injection molding of Stellite 6 powder: Sintering, microstructural and mechanical properties," *Materials Science and Engineering: A*, vol. 651, pp. 914-924, 1/10/ 2016.
- [2] P. Mariot, M. A. Leeflang, L. Schaeffer, and J. Zhou, "An investigation on the properties of injection-molded pure iron potentially for

- biodegradable stent application," *Powder Technology*, vol. 294, pp. 226-235, 6// 2016.
- [3] D. Y. Choi, S. Husein, and Y. G. Ko, "Influence of glass particles incorporation on the microstructure and magnetic properties of Fe-6.5wt% Si alloy subjected to metal injection molding technique," *Journal of Alloys and Compounds*, vol. 586, Supplement 1, pp. S305-S309, 2/15/ 2014.
- [4] R. L. S. B. Marçal, "Biomaterials Produced by Injection Molding," in *Reference Module in Materials Science and Materials Engineering*, ed: Elsevier, 2016.
- [5] M. R. Raza, A. B. Sulong, N. Muhamad, M. N. Akhtar, and J. Rajabi, "Effects of binder system and processing parameters on formability of porous Ti/HA composite through powder injection molding," *Materials & Design*, vol. 87, pp. 386-392, 12/15/ 2015.
- [6] M. M. Shbeh and R. Goodall, "Design of water debinding and dissolution stages of metal injection moulded porous Ti foam production," *Materials & Design*, vol. 87, pp. 295-302, 12/15/ 2015.
- [7] M. Aslam, F. Ahmad, P. S. M. B. M. Yusoff, K. Altaf, M. A. Omar, and R. M. German, "Powder injection molding of biocompatible stainless steel biodevices," *Powder Technology*, vol. 295, pp. 84-95, 7// 2016.
- [8] J.-P. Choi, G.-Y. Lee, J.-I. Song, W.-S. Lee, and J.-S. Lee, "Sintering behavior of 316L stainless steel micro-nanopowder compact fabricated by powder injection molding," *Powder Technology*, vol. 279, pp. 196-202, 7// 2015.
- [9] H. O. Gulsoy, S. Pazarlioglu, N. Gulsoy, B. Gundede, and O. Mutlu, "Effect of Zr, Nb and Ti addition on injection molded 316L stainless steel for bio-applications: Mechanical, electrochemical and biocompatibility properties," *Journal of the Mechanical Behavior of Biomedical Materials*, vol. 51, pp. 215-224, 11// 2015.
- [10] J. W. Oh, R. Bollina, W. S. Lee, and S. J. Park, "Effect of nanopowder ratio in bimodal powder mixture on powder injection molding," *Powder Technology*, vol. 302, pp. 168-176, 11// 2016.
- [11] J. Meng, N. H. Loh, G. Fu, S. B. Tor, and B. Y. Tay, "Replication and characterization of 316L stainless steel micro-mixer by micro powder injection molding," *Journal of Alloys and Compounds*, vol. 496, pp. 293-299, 4/30/ 2010.
- [12] W. Fang, X.-b. He, R.-j. Zhang, S.-d. Yang, and X.-h. Qu, "Evolution of stresses in metal injection molding parts during sintering," *Transactions of Nonferrous Metals Society of China*, vol. 25, pp. 552-558, 2015/02/01 2015.
- [13] M. R. Raza, F. Ahmad, N. Muhamad, A. B. Sulong, M. A. Omar, M. N. Akhtar, et al., "Effects of solid loading and cooling rate on the mechanical properties and corrosion behavior of powder injection

- molded 316 L stainless steel," *Powder Technology*, vol. 289, pp. 135-142, 2// 2016.
- [14] L. Gorjan, T. Kosmač, and A. Dakskobler, "Single-step wick-debinding and sintering for powder injection molding," *Ceramics International*, vol. 40, pp. 887-891, 1// 2014.
- [15] J. Song, J. C. Gelin, T. Barrière, and B. Liu, "Experiments and numerical modelling of solid state sintering for 316L stainless steel components," *Journal of Materials Processing Technology*, vol. 177, pp. 352-355, 7/3/ 2006.
- [16] M. A. Omar and I. Subuki, *Sintering Characteristics of Injection Moulded 316L Component Using Palm-Based Biopolymer Binder*: INTECH Open Access Publisher, 2012.